Biophysical Chemistry 151 (2010) 160–169

Contents lists available at ScienceDirect

Biophysical Chemistry

journal homepage: http://www.elsevier.com/locate/biophyschem

Hydration analysis of *Pseudomonas aeruginosa* cytochrome *c*551 upon acid unfolding by dielectric relaxation spectroscopy

Tetsuichi Wazawa [a,b], Takashi Miyazaki [a,b], Yoshihiro Sambongi [b,c], Makoto Suzuki [a,b,*]

[a] *Laboratory of Biomaterials Physical Chemistry, Department of Materials Processing, Graduate School of Engineering, Tohoku University, 6-6-02 Aobayama, Aoba-Ku, Sendai, Miyagi 980-8579, Japan*
[b] *CREST, JST, 4-19, Honcho, Kawaguchi, Saitama 332-0012 Japan*
[c] *Department of Molecular and Applied Biosciences, Graduate School of Biosphere Science, Hiroshima University, 1-4-4, Kagamiyama, Higashi-Hiroshima Hiroshima 739-8528, Japan*

ARTICLE INFO

Article history:
Received 6 May 2010
Received in revised form 21 June 2010
Accepted 22 June 2010
Available online 30 June2010

Keywords:
Dielectric dispersion
Debye relaxation
Loosely-bound water
Constrained water
Acid denaturation
Two-state transition

ABSTRACT

Dielectric relaxation (DR) study was performed to reveal the hydration change of *Pseudomonas aeruginosa* ferric cytochrome *c*551 (PA c551) in dilute aqueous solutions upon the acid unfolding which undergoes a two-state transition. The DR spectrum of a small spherical region containing a PA c551 molecule and its surrounding water shell was derived from the solution and solvent spectra by dielectric mixture theories. The derived spectrum was well-fitted with a sum of a Debye relaxation component (C1) with a DR frequency around 4.7 GHz and the bulk solvent component (CB). Upon acid unfolding, the DR amplitude of CB decreased with decreasing pH in an inverse manner to that of C1, while the total DR amplitude was almost constant. It indicates that C1 is due to the hydration water of PA c551. Little change in the DR frequency of C1 and a 1.7-fold increase in hydration number were observed.

1. Introduction

Hydration water is widely thought to affect the dynamics and conformation of proteins. Protein hydration has been extensively investigated by e.g., crystallography, magnetic relaxation dispersion, molecular simulation, and thermodynamic techniques [1–5]. Although hydration water is undoubtedly concerned with the functions and folding of proteins, quantitative understanding of hydration changes upon such processes has still been remained insufficient. Dielectric relaxation spectroscopy (DRS) is a technique to measure the electric response of a sample material experiencing an oscillating electric field of small amplitude. It can be applied to a wide variety of samples without molecular probes like isotopes, fluorescent dyes, spin labels, and so on. The frequency dependence of the complex dielectric permittivity of a sample provides detailed information of dynamic processes involved in the polarizable components, e.g., rotational relaxation of water molecules, ion cloud relaxation, ion pair rotation, and intramolecular structural relaxation [6]. Through the analysis of the dielectric relaxation (DR) spectra of dielectric sample materials such as aqueous protein solutions, their dynamic processes are able to be resolved with respect to their corresponding time scales. Thus, DRS is a powerful technique to investigate protein hydration.

Recently-commercialized computerized vector network analyzers have powered DRS studies [7], and enabled us to measure DR spectra over a frequency range from 10^8 to 0.5×10^{11} Hz in tens of seconds at high accuracy or reproducibility around 0.5–1% in dielectric permittivity. Further improvement has been achieved by our group to realize even higher reproducibility of 0.025% in dielectric permittivity over the frequency range from 1 to 26 GHz [8]. This enables us to resolve 2.2% difference in $\log_{10} f_c$, where f_c is the DR frequency of hydration water of protein in solution as dilute as 10 mg·mL^{-1}. Therefore, high-resolution measurements of DR spectra of aqueous protein solutions can be conducted in various experimental configurations and conditions in a high throughput manner.

By the DRS measurements of protein solutions, several dielectric dispersions are observed, and they are called β, δ, and γ-dispersions [9]. The β-dispersion is known to occur around 1 MHz at room temperature and assigned to protein tumbling [10], and the γ-dispersion, at ~17 GHz at 20 °C and assigned to cooperative reorientation of bulk water molecules [11]. Importantly, previous DRS studies of aqueous protein solutions revealed a dielectric dispersion arising from the hydration water of protein, δ-dispersion the DR frequency range from 3 to 10 GHz. The relaxation frequencies were several-fold lower than that of bulk water [9,12,13]. Such hydration water with the lowered DR frequency is called loosely-bound water or constrained water. So far, studies on the constrained

* Corresponding author. Laboratory of Biomaterials Physical Chemistry, Department of Materials Processing, Graduate School of Engineering, Tohoku University, 6-6-02 Aobayama, Aoba-Ku, Sendai, Miyagi 980-8579, Japan. Tel./fax: +81 22 795 7303.
E-mail address: msuzuki@material.tohoku.ac.jp (M. Suzuki).

0301-4622/$ – see front matter © 2010 Elsevier B.V. All rights reserved.
doi:10.1016/j.bpc.2010.06.008

water of proteins in aqueous solution were carried out to understand thermodynamic stability and functions of proteins such as myoglobin, ribonuclease A, hemoglobin, horse heart cytochrome *c*, bovine serum albumin, ovalbumin and ubiquitin [13–19]. Our studies on aqueous actin filament solutions demonstrated the presence of the hypermobile water in addition to the constrained water [20,21]. Thus, high-resolution microwave DRS can provide a new tool to characterize hydration water of proteins quantitatively, and therefore, the DRS is promising to give clear insights into protein folding mechanism and enzymatic functions. In particular, currently, the whole process of acid unfolding of protein can be revealed by the present study, by further advancing our former study of acid-unfolded and molten globule states of apomyoglobin [22].

In this study, we have investigated aqueous solutions of *Pseudomonas aeruginosa* cytochrome *c*551 (PA c551) by the microwave DRS for the first time over the pH range from 1 to 6, in which PA c551 undergoes acid unfolding. PA c551 is an extensively-studied class I bacterial cytochrome *c* and composed of 82 amino acids and protoheme [23]. The structure of PA c551 was resolved by X-ray crystallography and NMR [24,25]. The thermal, denaturant-induced and acid-induced unfolding of PA c551 and its variants were also studied [26–29]. An equilibrium unfolding study showed that the acid unfolding of PA c551 was a one-step reaction with a pK_a value of 1.8, and thereby, heme misligation did not occur during the acid unfolding reaction [29]. Therefore, the acid unfolding of PA c551 was investigated in the study. Moreover, the low concentration of acid to induce its acid unfolding gives rise to low background noise in DRS measurements. In contrast, high concentration of denaturants (>1 M) often causes high background noise in DR spectra, although denaturant-induced unfolding experiments generally require such high concentrations. Herein, we measured the microwave DR spectra of aqueous PA c551 solutions in the acidic pH range with sulfuric acid since it is less corrosive to the microwave probes and electric parts.

2. Materials and methods

2.1. Preparation of PA c551

PA c551 was expressed in *E. coli* and extracted by the cold osmotic shock technique as reported previously [25]. The details of ferric PA c551 purification are provided in Supplementary material A1. Prior to DRS measurement, the purified ferric PA c551 was concentrated (9–15 mg mL^{-1}, unless mentioned), thoroughly dialyzed against a H_2SO_4 solution (for pH 1.0–1.3) or a solution containing H_2SO_4 and Na_2SO_4 ($[H_2SO_4]+[Na_2SO_4]=30$ mM; as a nonvolatile less-corrosive buffer than a chloride system for the dielectric probe in the pH range 1.8–6.2), and then, ultra-centrifuged at 230,000×*g* for 10 min at 4 °C to remove some aggregate. The pH of the solution was adjusted by changing the ratio $[H_2SO_4]$:$[Na_2SO_4]$. The supernatant solution and the dialysates were used to measure the DR spectra of the PA c551 solution and a reference solvent, respectively.

2.2. Measurement of DR spectra

DRS measurement was performed on a vector network analyzer (PNA8364B; Agilent, Santa Clara, CA) equipped with an Electric Calibration Kit (N4691A, Agilent), a High Temperature Dielectric Probe Kit (85070E-020, Agilent) and an in-house fabricated conical glass cell (volume, 4 mL) into which sample solution was introduced. Materials Measurement Software (85070E, Agilent) was used to control the network analyzer and to measure DR spectra given by,

$$\varepsilon^*(f) = \varepsilon'(f) - i\varepsilon''(f), \tag{1}$$

where ε' and ε'' are, respectively, the real part and negative imaginary part of the complex dielectric permittivity, f is a microwave frequency (0.2–26 GHz), and $i^2=-1$. The details of the DRS measurements are provided in Supplementary material A2.

The glass cell attached with the dielectric probe was soaked in a bath filled with water the temperature of which was controlled at 20.00±0.01 °C using a refrigerated bath circulator (NESLAB RTE-17; Thermo Fisher Scientific, Waltham, MA). The vector network analyzer was calibrated with the responses of the dielectric probe in air, short-circuited and immersed in pure water at 20.00 °C. The DRS measurement was performed in the frequency range of 0.2–26 GHz with logarithmically-spaced 301 frequency points. Every sample solution was degassed prior to measurement to prevent the generation of air bubbles on the dielectric probe surface, which gave rise to noise in the DR spectrum.

The DRS data of the aqueous solutions were processed according to ref [8] with slight modification. The DR spectra of the aqueous PA c551 solution and the reference solvent, each of which was the average of consecutively-acquired five (or more) raw data, were alternately recorded in pairs 6 times or more. The DR spectra of the PA c551 solution $\varepsilon^*_{ap,raw}$ and the reference solvent $\varepsilon^*_{w,raw}$ are shown in Fig. 1a. The net dielectric permittivity of the reference solvent $\varepsilon^*_{w,raw}$ was divided into two terms by

$$\varepsilon^*_{x,raw}(f) = \varepsilon^*_x(f) + i\frac{\sigma_x}{2\pi f\varepsilon_0} \quad (x = w,ap), \tag{2}$$

where ε_0 is the permittivity in vacuum, and σ_x is the electric conductivity of solvent (w) or solution (ap) which was initially adjusted so that ε''_w (0.2 GHz) = 1.0 (Fig. 1a) and finally determined by the cross recursive analysis as provided in Supplementary material A3.

2.3. Analysis of the dielectric property of the hydration shell of PA c551

We assumed that PA c551 molecules in the native state (N state) or unfolded state (U state) are monodispersed in the solvent. As shown in Supplementary material A4 and Supplementary Fig. A1, the difference dielectric permittivity between the PA c551 solution and its reference solvent exhibited proportionality with respect to protein concentration below 23 mg·mL^{-1} in the frequency range from 0.2 to 26 GHz, and this underpins the monodispersion condition. In the present analysis, a dielectrically equivalent (spherical or ellipsoidal) particle was taken to substitute the spherical or ellipsoidal region containing a PA c551 molecule and the surrounding water [13,16,30–33]. Since the PA c551 molecules were observed to be monodispersed in the solvent (see above), dielectric mixture theories [31–33] were used to derive the DR spectrum of the dielectric particle, $\varepsilon^*_q(f)$, at a given volume fraction ϕ.

The DR spectrum $\varepsilon^*_q(f)$ of a particle containing a PA c551 molecule and the surrounding solvent water was fitted with two Debye-type DR functions and the bulk solvent component given by $(\varepsilon^*_w(f)-\varepsilon^*_{w,\infty})$ (see Fig. 2, Supplementary material A3). One of the two Debye components was attributed to the hydration water of the protein [12,13,16,17], and the DR frequency was ~5 GHz. Additionally, bulk water exhibits a DR frequency of 17 GHz at 20 °C [11]. Thus, we denote by an A-particle a dielectric particle composed of a PA c551 and the hydration and bulk water surrounding PA c551, which shows dielectric dispersions in the high frequency region of >3 GHz (Fig. 2a). Here, we designate the DR spectrum of the A-particle corresponding to a volume fraction of ϕ_A by $\varepsilon^*_{q,A}(f)$. The rest of the two Debye type components was found to show a DR frequency of ~0.2 GHz, and would be attributed to fluctuation of the ion cloud around charged groups of peptide chains [34] or fluctuation of polypeptide chains [18,35] responding to AC electric field in the solvent water (Fig. 2a). For simplicity in analysis, we assumed that the latter polarizable components (ionic clouds or polar polypeptide chains) were substituted by dielectric particles, say B-particles, and also assumed

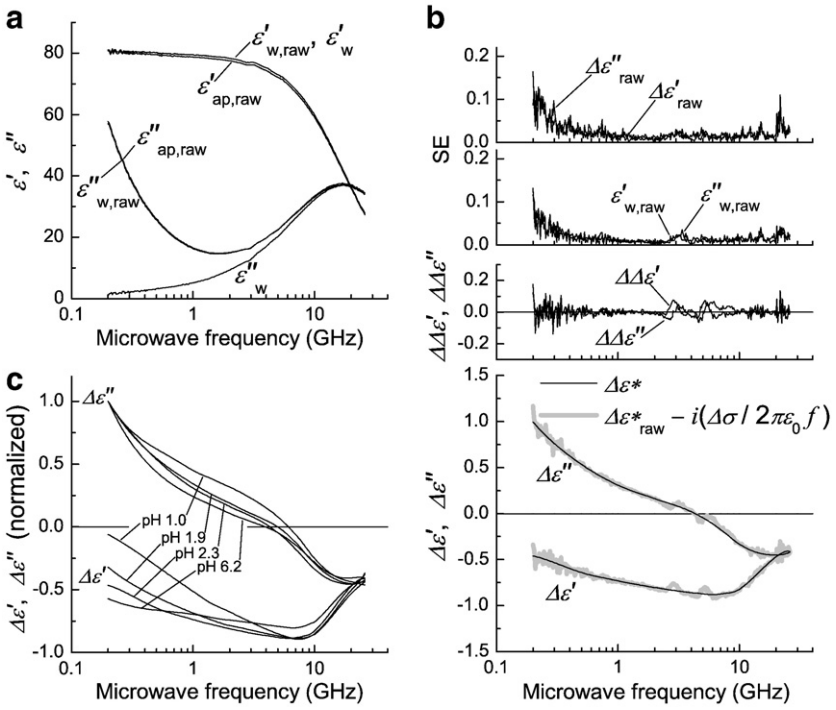

Fig. 1. DR spectra of PA c551 solution and its solvent at 20.0 °C. (a) The raw spectra of the PA c551 solution ($\varepsilon^*_{ap,raw}$) and the solvent ($\varepsilon^*_{w,raw}$). The DR spectrum of the solvent which was subtracted by the electric conduction term is also shown (ε^*_w). The solvent is an aqueous solution containing 4.9 mM H_2SO_4 and 25.1 mM Na_2SO_4 (pH 2.3): PA c551 concentration, 9.92 mg mL^{-1}. (b) The difference spectrum of the PA c551 solution and the reference solvent before ($\Delta\varepsilon^*_{raw}$) and after ($\Delta\varepsilon^*$) smoothing (bottom panel). The top panel shows the standard errors (SE) of $\Delta\varepsilon'_{raw}$, $\Delta\varepsilon''_{raw}$, $\varepsilon'_{w,raw}$, and $\varepsilon''_{w,raw}$ ($n=30$). The middle panel shows the difference $\Delta\Delta\varepsilon^* = \Delta\varepsilon^*_{raw} - i\Delta\sigma/2\pi\varepsilon_0 f - \Delta\varepsilon^*$. (c) The real and imaginary parts of the smoothed difference spectra ($\Delta\varepsilon^*$) of PA c551 at pH 1.0, 1.9, 2.3 and 6.2. For comparison, the spectra are normalized to 10 mg mL^{-1} by multiplying a factor of $10/c$, where c is the protein concentration (mg·mL^{-1}). The complex dielectric permittivity is given as $\varepsilon^* = \varepsilon' - i\varepsilon''$. For the definition of the symbols used in (a–c), see text and Supplementary material A2.

that they were monodispersed and mixed in the solvent apart from the A-particles. We denote by $\varepsilon^*_{q,B}(f)$ the DR spectrum of the B-particles with its volume fraction ϕ_B.

The cross-recursive procedure was used to analyze the DR components in PA c551 solutions (Fig. 2b–d). The details of the analysis are provided in Supplementary material A3**.** Firstly, the DR parameters of the A-particles were coarsely obtained (Fig. 2b). The dielectric spectrum $\varepsilon^*_q(f)$ of a particle mixed in a solvent with $\varepsilon^*_r(f)$ was obtained by Wagner's equation [31],

$$\varepsilon^*_q = \varepsilon^*_r \frac{2(1-\phi)\varepsilon^*_r - (2+\phi)\varepsilon^*_{ap}}{(1-\phi)\varepsilon^*_{ap} - (1+2\phi)\varepsilon^*_r}, \tag{3}$$

where $\varepsilon^*_{ap} = \Delta\varepsilon^* + \varepsilon^*_w$ (Supplementary material A2) and ϕ is the volume fraction of the mixed particles. Then the dielectric spectrum of A-particles $\varepsilon^*_q(f) = \varepsilon^*_{q,A}(f)$ was calculated at a given volume fraction ϕ_A by letting $\varepsilon^*_r = \varepsilon^*_w$. The spectrum $\varepsilon^*_{q,A}(f)$ was then fitted with a model function,

$$\varepsilon^*_{q,\mathrm{model},A}(f) = \varepsilon_{q,\infty} + \alpha(\varepsilon^*_w(f) - \varepsilon_{w,\infty}) + \frac{\delta_{A1}}{1 + i\frac{f}{f_{c,A1}}}, \tag{4}$$

to obtain the best values of $f_{c,A1}$, δ_{A1}, and α, which are, respectively, the DR frequency, DR amplitude and the fraction of bulk solvent contribution, and the least squares fitting was performed in the range of 3–26 GHz. Due to this limitation of frequency range, this least squares fitting mainly evaluated the dielectric dispersions of the A-particle, and thereby, the Debye-type relaxation term in Eq. (4) usually fell into the dielectric dispersion around 5 GHz, attributed to the hydration water. By sweeping the volume fraction ϕ, we could find a volume fraction ϕ_{HB} such that the least squares fitting gave zero of the fraction of bulk solvent contribution α at $\phi_A = \phi_{HB}$, which means the volume fraction of the hydration water/bulk water boundary [8]. Thus, the DR frequency and amplitude, $f_{c,HB}$ and δ_{HB}, respectively, were derived at the volume fraction ϕ_{HB}, the DR spectrum of this A-particle at $\phi = \phi_{HB}$ was obtained by $\varepsilon^*_{q,\mathrm{model,HB}}(f) = \varepsilon_{q,\infty} + \delta_{HB}/(1 + if/f_{c,HB})$, and then, a DR spectrum, designated by $\varepsilon^*_{w,A}$, of a conceptual solution containing only the A-particles of $\varepsilon^*_{q,\mathrm{model,HB}}$ dissolved in the reference solvent was simulated by Eq. (3) (let $\varepsilon^*_r = \varepsilon^*_w$, $\varepsilon^*_q = \varepsilon^*_{q,\mathrm{model,HB}}$, and $\phi = \phi_{HB}$, then solve ε^*_{ap}) (Fig. 2b).

Secondly, to determine the DR parameters of the B-particle, the DR spectrum $\varepsilon^*_{q,B}(f)$ was computed at a predefined value of volume fraction ϕ_B from the spectra of ε^*_{ap} and $\varepsilon^*_{w,A}$ by Eq. (3) after replacing ϕ to ϕ_B (Fig. 2c). The DR spectrum $\varepsilon^*_{q,B}(f)$ was then fitted with a model function

$$\varepsilon^*_{q,\mathrm{model,B}}(f) = \varepsilon^*_w(f) + \frac{\delta_B}{1 + i\frac{f}{f_{c,B}}}, \tag{5}$$

to obtain the best values of the DR frequency and amplitude, $f_{c,B}$ and δ_B, respectively, of the Debye-type increment above the spectrum of bulk solvent. This least squares fitting was performed in the frequency range of 0.2–3 GHz to exclusively derive the DR parameters of the B-particles. Furthermore, the DR spectrum, designated by $\varepsilon^*_{w,B}$ of a conceptual solution containing only the B-particles of $\varepsilon^*_{q,\mathrm{model,B}}$ dissolved in the reference solvent was simulated by Eq. (3) with the volume fraction ϕ_B.

Thirdly, to more accurately determine the DR parameters of A-particles, the DR spectrum $\varepsilon^*_{q,A}$ was obtained from the spectra of ε^*_{ap} and $\varepsilon^*_{w,B}$ (Fig. 2d). Using the DR spectrum of $\varepsilon^*_{q,A}$, in place of ε^*_q, the procedure of the determination of ϕ_{HB} and $\varepsilon^*_{q,\mathrm{model,HB}}$ described above was performed. Because the contribution of the B-particle was removed in the DR spectrum $\varepsilon^*_{q,A}$, the DR parameters derived from $\varepsilon^*_{q,A}$ should be improved. After computing the spectrum $\varepsilon^*_{w,A}$ from $\varepsilon^*_{q,\mathrm{model,HB}}$ and ε^*_w at the volume fraction ϕ_{HB}, the procedure for

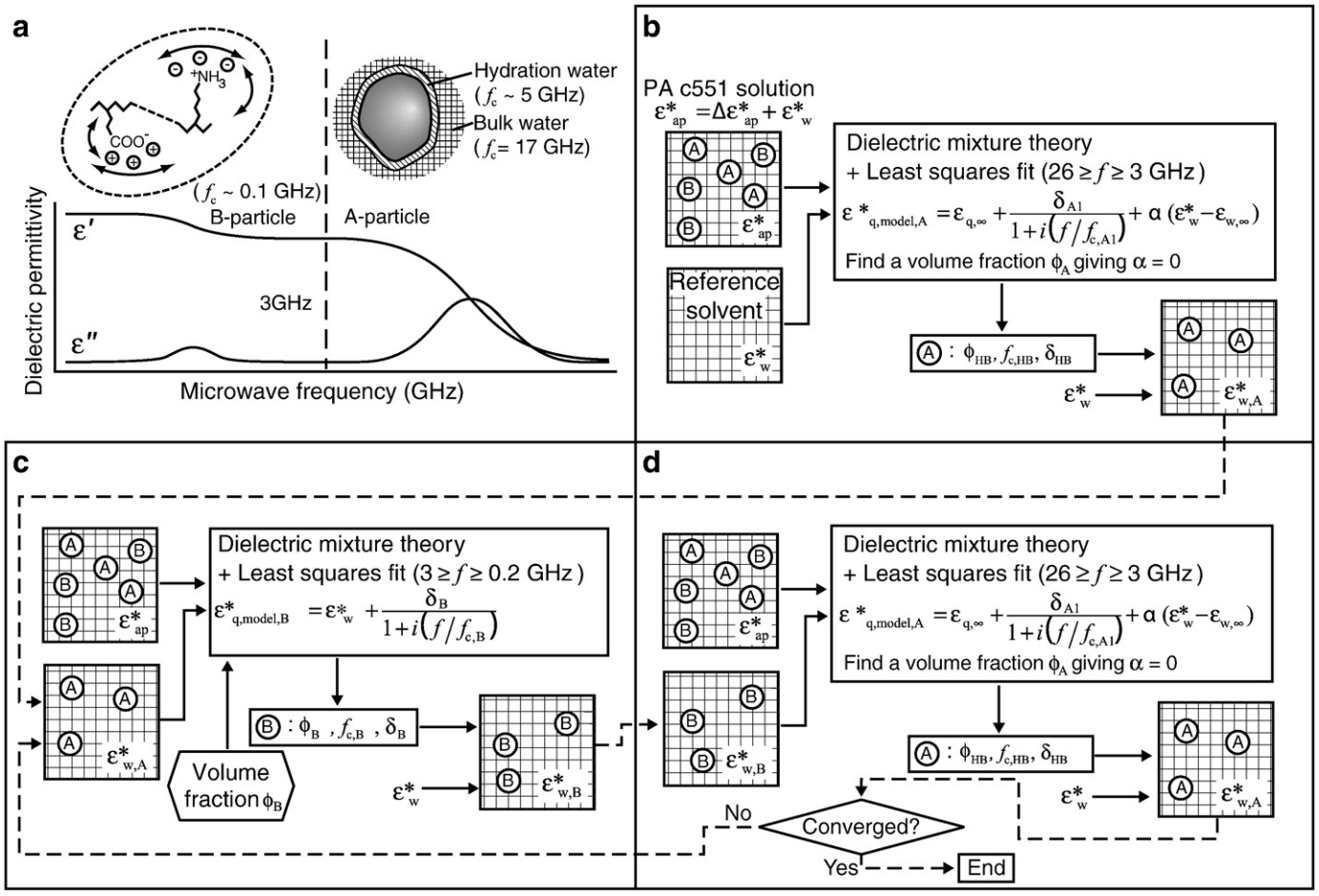

Fig. 2. Schematic illustration of the relaxation component analysis of DR spectra. (a) The dynamic processes under the coverage of the present DRS study. In the DR spectra of PA c551 solutions, dielectric relaxations attributed to the cooperative reorientation of the bulk and hydration water around PA c551 molecules are observed in the range of ≥3 GHz, and the ensemble of the components are denoted by A-particles. A dielectric relaxation probably due to ion clouds relaxation and/or structural fluctuation in PA c551 molecules is observed in the range of ≤3 GHz, and the polarizing component is denoted by B-particles. (b–d) The flow of the cross-recursive analysis of the DR spectra. (b) Coarse determination of the DR parameters of the A-particle. (c) The determination of the DR parameters of the B-particle from ε^*_{ap} and $\varepsilon^*_{w,A}$ derived in panel (b). (d) The determination of the DR parameters of the A-particle from ε^*_{ap} and $\varepsilon^*_{w,B}$ derived in panel (c). For detail, see the text and Supplementary material A3.

the B-particles (see above) was conducted using $\varepsilon^*_{w,A}$ for more accurate determination. Likewise, the procedures for the A- and B-particles were alternately iterated until the DR parameters for both particles reached convergence.

In Fig. 3a, the DR spectra of $\varepsilon^*_{q,A}$ at $\phi_A = \phi_{HB}$ and $\varepsilon^*_{q,model,HB}$ are shown. Although the least squares fitting of $\varepsilon^*_{q,model,HB}(=\varepsilon^*_{q,model,A}$ at $\phi_A = \phi_{HB}$, by definition) with $\varepsilon^*_{q,A}(f)$ was performed using only their real parts (Supplementary material A3.2), the simulated spectrum $\varepsilon^*_{q,model,HB}$ shows a good agreement with the imaginary part $\varepsilon''_{q,A}$ as well as the real part $\varepsilon'_{q,A}$ in the frequency range of 3–26 GHz in which the value of χ^2_1 (Eq. (7) in Supplementary material A3) was evaluated. In Fig. 3b, the DR spectra of $\varepsilon^*_{q,B}(f)$ and $\varepsilon^*_{q,model,B}(f)$ at $\phi_B/c = 0.00731\ mg^{-1}\cdot mL$ are shown, where c is the concentration of PA c551. Noting that the static dielectric permittivity of pure water is 80.4 at 20 °C [11], the increments of the spectra of $\varepsilon'_{q,B}(f)$ above the dielectric permittivity of the reference solvents (Eq. (5)) are clearly noticeable at low frequencies below 1 GHz. The simulated spectrum $\varepsilon^*_{q,model,B}(f)$ was found to fit to the spectrum $\varepsilon^*_{q,B}(f)$ in the low frequency range below 3 GHz (Fig. 3b). Furthermore, Fig. 3c shows the DR spectrum of a mixture such that B-particles of $\varepsilon^*_{q,model,B}$ and A-particles of $\varepsilon^*_{q,model,A}$ are suspended in the reference solvent at volume fractions of $\phi_B/c = 0.00731\ mg^{-1}\cdot mL$ and ϕ_{HB}, respectively. This simulated spectrum gives a good description of $\varepsilon^*_{ap} = \Delta\varepsilon^* + \varepsilon^*_w$, as expected.

Furthermore, once the volume fraction of the hydration boudary ϕ_{HB} is determined, one can evaluate the number of water molecules which constitute the hydration shell. The number of the hydration water molecules N_{hyd} was calculated by

$$N_{hyd} = \frac{55.6(\phi_{HB} - \xi)}{c_m}, \tag{6}$$

where $c_m = c/M_w$ is the molar concentration in mol L^{-1} of PA c 551. It should be noted that the value ϕ_{HB} is much more sensitive to the solute volume than the solute shape as discussed in Section 3.5.

2.4. The mixture theory of dielectric ellipsoids

To investigate the effect of the shape of solute molecule on the DR parameters, a dielectric mixture theory for ellipsoids [32,33], in place of the Wagner's theory, was also employed. The equation is given by

$$\frac{\varepsilon^*_{ap} - \varepsilon^*_w}{\varepsilon^*_{ap} + 2\varepsilon^*_w} = \frac{\phi}{9}\sum_{k=x,y,z}\frac{\varepsilon^*_q - \varepsilon^*_w}{\varepsilon^*_w + (\varepsilon^*_q - \varepsilon^*_w)L_k} \tag{7}$$

where L_k is a depolarization factor which is dependent on an axial ratio $q = R_z/R_x$. Here, the surface of the ellipsoid is expressed as $(x/R_x)^2 + (y/R_y)^2 + (z/R_z)^2 = 1$, where R_x, R_y and R_z are the semiaxes

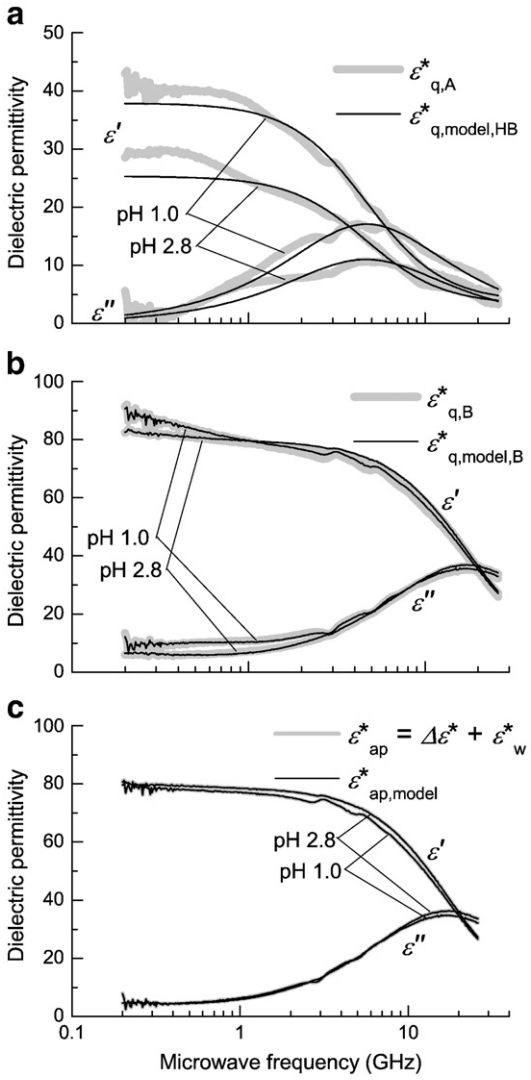

Fig. 3. DR spectra of PA c551 solutions and their simulated DR spectra. (a) DR spectrum of $\varepsilon^*_{q,A}$ at a volume fraction of ϕ_{HB} and $\varepsilon^*_{q,model,HB}$ (Eqs. (3) and (4)): volume fractions of hydration boundary ϕ_{HB}, 0.0129 and 0.0160 for pH 2.8 and 1.0, respectively. The deviations below 3 GHz appear outside of the fitting range between 3 to 26 GHz for $\varepsilon^*_{q,A}$. (b) DR spectrum of $\varepsilon^*_{q,B}$ and $\varepsilon^*_{q,model,B}$ (Section 2.3, Eq. (5)): volume fractions ϕ_B, 0.0913 and 0.0895 for pH 2.8 and 1.0, respectively. (c) The experimental DR spectra of the whole PA c551 solution ε^*_{ap}were almost perfectly simulated by $\varepsilon^*_{ap,model}$. The spectra of $\varepsilon^*_{ap,model}$ were computed using an equation derived from the Wagner's mixture theory given by $\frac{\varepsilon^*_{ap,model}-\varepsilon^*_w}{\varepsilon^*_{ap,model}+2\varepsilon^*_w} = \phi_{HB}\frac{\varepsilon^*_{q,model,HB}-\varepsilon^*_w}{\varepsilon^*_{q,model,HB}+2\varepsilon^*_w} + \phi_B\frac{\varepsilon^*_{q,model,B}-\varepsilon^*_w}{\varepsilon^*_{q,model,B}+2\varepsilon^*_w}$: PA c551 concentration, 12.5 and 12.2 mg·mL^{-1} for pH 2.8 and 1.0, respectively.

along x-, y- and z-axes, respectively, and $R_x = R_y$. The value of $\varepsilon_{q,\infty}$ for ellipsoidal model was calculated according to ref [20].

3. Results

3.1. pH dependence of the absorbance spectrum of PA c551

To examine the conformational change of ferric PA c551, its absorbance spectrum was measured in the acidic to neutral pH range (Fig. 4a). The protocol of this measurement is provided in Supplementary material A5. The spectrum was typical of the low spin state of heme for pH ≥ 2.3, whereas typical of the high spin state for pH ≤ 1 [36]. The spectra exhibited isosbestic points at 483, 509, 589 and 649 nm for pH ≥ 0.7 (Fig. 3a), indicating that the transition between the high and low spin states is most likely to be a two-state transition. As a representative wavelength point, the absorbance at 532 nm is plotted as a function of pH (Fig. 4b). Importantly, the pH change of the

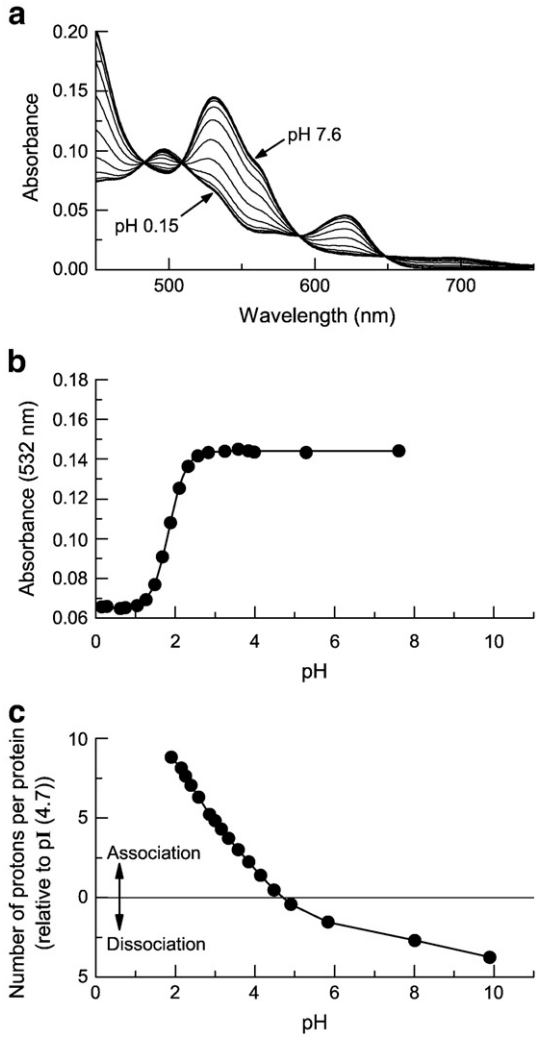

Fig. 4. The absorbance spectra for pH-titration of PA c551 at 20.0 °C. (a) The absorbance spectra of PA c551 from pH 0.15 to 7.6 are shown. (b) The absorbance at 532 nm was plotted as a function of pH. The simulated absorbance A_{sim} based on a single cooperative acid unfolding (Eq. (8)) was drawn using the pK_a and n_H values of 1.8 and 2.1. (c) Acid/base titration of PA c551 at 20.0 °C. The number of association and dissociation of protons per protein molecule is plotted versus pH. The amount is shown as a relative value to the isoelectric point, 4.7 (see Supplementary material A6): PA c551 concentration, 7.90 mg mL^{-1}.

absorbance satisfactorily fits with a single cooperative transition model of $N + n_H H^+ \rightleftarrows U$ given by

$$A_{sim} = A_{High}\frac{[H^+]^{n_H}}{[H^+]^{n_H} + K_a^{n_H}} + A_{Low}\frac{K_a^{n_H}}{[H^+]^{n_H} + K_a^{n_H}}, \quad (8)$$

where A_{sim}, A_{High}, A_{Low}, K_a and n_H are the simulated absorbance, absorbance at the high spin state, absorbance at the low spin state, dissociation constant, and Hill coefficient, respectively. The fitting with the single cooperative transition yielded pK_a and n_H of 1.8 and 2.1, respectively. These values are consistent with the results by Bigotti et al. [29]. In this study, the conformational states of PA c551 for pH ≤ 1 and pH ≥ 2.3 are referred to as the acid-unfolded (U) and native (N) states, respectively.

3.2. pH dependence of the DR property of the hydration shell of PA c551

The cross-recursive analysis of the DR spectrum of PA c551 solution using the Wagner's dielectric mixture theory (Section A3.3 of

Supplementary material A3) and the least squares fitting with the model function Eq. (4) allowed us to determine the hydration water/bulk water boundary designated at the hydration boundary volume fraction $\phi_A = \phi_{HB}$, the DR frequency $f_{c,HB}$, the DR amplitude δ_{HB}, and the number of hydration water molecules N_{hyd} (Eq. (6)). Here, we employed the Wagner's theory [31] to analyze the DR spectra of PA c551 solution over the pH range of 1.0–6.2 irrespective of pH-dependent conformations of PA c551. Thus, $f_{c,HB}$, δ_{HB} and N_{hyd} were determined as a function of pH (Fig. 5). Fig. 5a shows that $f_{c,HB}$ seems unchanged within the measurement error between pH 1.0 and 2.8 and the mean value is 4.69 GHz, whereas it obviously increases with pH from 2.8 to 6.2. Likewise, the pH change of δ_{HB} is separated into two regimes: δ_{HB} rapidly decreases with pH from 1.0 to 2.3 and stays almost constant for pH 2.3–6.2 (Fig. 5b). The dielectric dispersion around 5 GHz has been observed in the DR spectra of aqueous solutions of various proteins, and known to be attributed to the hydration water surrounding the proteins [12,13,16–18]. A plot of $f_{c,HB}$ versus δ_{HB} more evidently demonstrates the two regimes of the pH-dependent DR property: for pH 1.0–2.3, $f_{c,HB}$ is constant but δ_{HB} decreased with pH increase; for pH 2.3–6.2, $f_{c,HB}$ slightly increased with pH increase but δ_{HB} was almost constant (Fig. 5c). Additionally, Fig. 5d shows a significant change of N_{hyd} in the lower pH range, but little change for pH>2.3. Thus, the present hydration analysis using DRS successfully determined the DR property and the amount of the hydration water surrounding PA c551.

Interestingly, the absorbance spectrum of PA c551 was unchanged and therefore PA c551 was in the native state between pH 2.3 and 6.2 (Fig. 4a), whereas the DR frequency $f_{c,HB}$ of the hydration shell was found to increase with the pH increase (Fig. 5a). This increase of $f_{c,HB}$ probably reflects the increase of the rotational mobility of the hydration water of PA c551. By acid/base titration of PA c551, a release of 10 protons from one PA c551 molecule was observed when pH was increased from 2 to 6. (Fig. 4c and Supplementary material A6). Thus, the ionization of the surface residues of PA c551 may be responsible for the change of the increase of the DR frequency.

3.3. pH dependence of the dielectric dispersion at the lower frequency

The cross-recursive analysis of the DR spectra of PA c551 solutions described above at the same time derived the DR parameters for the low frequency component of dielectric dispersion around 0.2 GHz, i.e.,

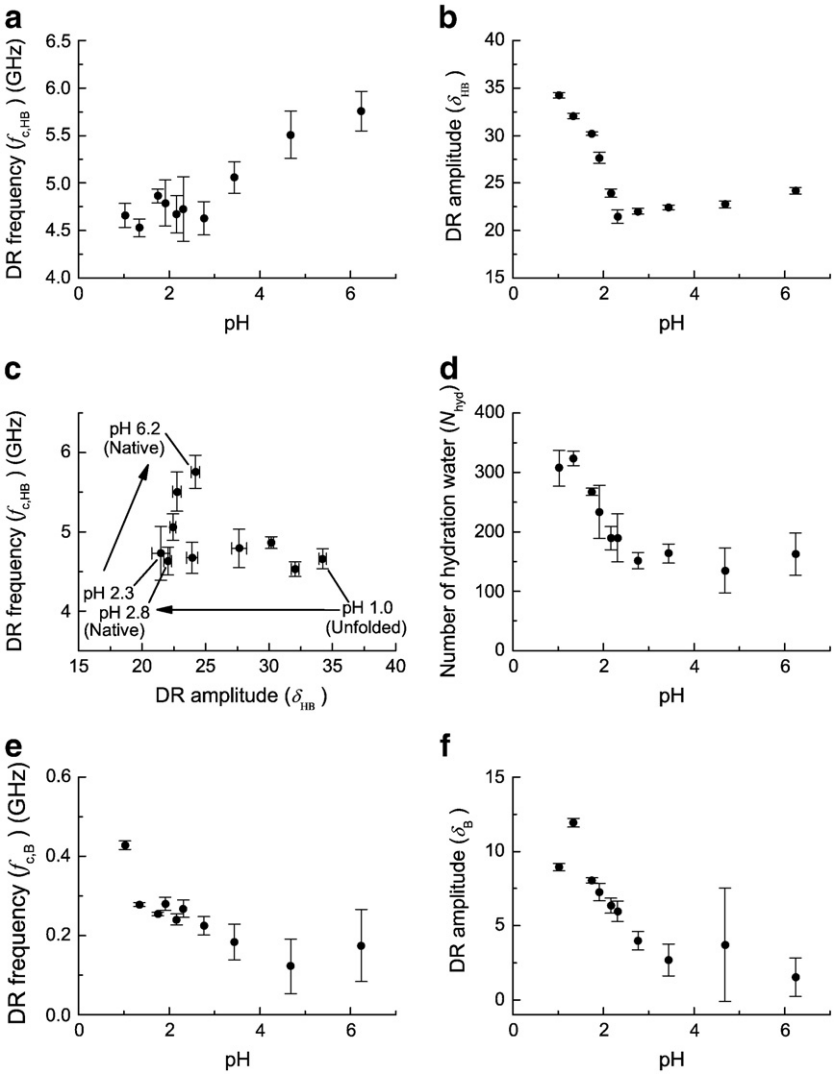

Fig. 5. The pH dependences of the DR frequency, the DR amplitude, and the number of hydration water of the dielectric particle at $\phi_A = \phi_{HB}$. (a) DR frequency $f_{c,HB}$ vs pH. (b) DR amplitude δ_{HB} vs pH. (c) $f_{c,HB}$ vs δ_{HB}. (d) The number of hydration water N_{hyd} computed by Eq. (6) was plotted against pH. The error bars represent the calculated errors by the error propagation theory from the standard errors in $\varepsilon^*_{w,raw}$ and $\varepsilon^*_{ap,raw}$ to the DR parameters. (e) The DR frequency for the dielectric dispersion corresponding to B-particle, $f_{c,B}$. (f) The DR amplitude for the dielectric dispersion corresponding to B-particles, δ_B. All the DR parameters were determined by the cross-recursive analysis at $\phi_B/c = 0.00731\ mg^{-1}\cdot mL$ (see Supplementary material A3).

the B-particles. This component was, by a good approximation, examined as a Debye-type increment above the dielectric permittivity of bulk solvent (Fig. 3b; Section A3.4 of Supplementary material A3). The DR frequency and amplitude of this component, $f_{c,B}$ and δ_B, respectively, were obtained at a fixed ϕ_B/c value of 0.0073 mg^{-1} mL as a function of pH (Fig. 5e,f). As shown in Fig. 5e, the DR frequency $f_{c,B}$ ranges between 0.12 and 0.27 GHz between pH 1.3 and 6.2, albeit $f_{c,B}$ at pH 1.0 shows a somewhat higher value of 0.43 GHz. Importantly, the DR amplitude δ_B (Fig. 5f) shows a concurrent pH dependence with that of the hydration water (Fig. 5d): the value of δ_B decreased by ~3-fold with pH from pH 1 to 3 and stays almost constant for pH>3. This agreement of the pH range for the changes of the DR amplitudes, δ_{HB} and δ_B, suggests that the dielectric dispersion around 0.2 GHz reflects the extension of the peptide chain of PA c551 and its concomitant alteration of the microenvironment of PA c551 such as counter ionic clouds.

3.4. Hydration analysis on a fixed volume containing a protein molecule

The DR spectrum of a particle with a fixed volume per PA c551 molecule containing a PA c551 molecule and its surrounding water was analyzed between pH 1.0 and 2.8. This analysis procedure allowed us to quantitatively investigate how the DR amplitude δ_{A1} and the fraction of bulk solvent contribution α changed within the particle of fixed volume upon acid unfolding. Additionally, in this analysis, the DR frequency was fixed at 4.69 GHz, the mean value of $f_{c,HB}$ in the range of pH 1.0–2.8 in Fig. 5a, since $f_{c,HB}$ was almost unchanged within the measurement error in this pH range. Thus, $\varepsilon_q^*(f)$ was derived by using the Wagner's equation (Eq. (3)), letting $\varepsilon_r^* = \varepsilon_w^*$, and using a fixed values of $f_{c,A1} = 4.69$ and ϕ_A /c, where c is a concentration of PA c551, and then, the least squares fitting analysis was performed (see Sections A3.2 of Supplementary material) to obtain the DR amplitude δ_{A1} and the fraction of bulk solvent contribution α. In Fig. 6, the values of δ_{A1} and α derived through this procedure at $\phi_A/c = 0.00423$ mL·mg^{-1} are plotted as a function of pH. The value of $\phi_A/c = 0.00423$ mL mg^{-1} was higher than any of the ϕ_{HB}/c values obtained in this study. Importantly, the DR amplitude δ_{A1} decreased with pH increase, whereas the fraction of bulk solvent contribution α increased with pH (Fig. 6). This result indicates that the increase of the DR amplitude δ_{A1} of the 4.69-GHz component upon acid unfolding is due to the increase of the hydration water of PA c551 transformed from bulk water. The pH changes of the DR amplitude δ_{A1} and the fraction of bulk solvent contribution α (Fig. 6) were simulated as a single cooperative transition between U and N states. Here, we model the DR amplitude δ_{sim} and the fraction of bulk solvent contribution α_{sim} with a single cooperative transition expressed by

$$\delta_{sim} = \delta_0 \frac{[H^+]^{n_H}}{[H^+]^{n_H} + K_a^{n_H}} + \delta_1 \frac{K_a^{n_H}}{[H^+]^{n_H} + K_a^{n_H}}, \quad (9)$$

and

$$\alpha_{sim} = \alpha_0 \frac{[H^+]^{n_H}}{[H^+]^{n_H} + K_a^{n_H}} + \alpha_1 \frac{K_a^{n_H}}{[H^+]^{n_H} + K_a^{n_H}}, \quad (10)$$

respectively, where δ_0 and δ_1 are the DR amplitudes at high and low pH limits, respectively, and α_0 and α_1 are the fractions of bulk solvent contribution at high and low pH limits, respectively. The models expressed by Eqs. (9) and (10) were found to be well fitted to the data points (Fig. 6). The plot of δ versus pH yielded pK_a and n_H values of 1.9 and 2.5, respectively, and the plot of α, 1.9 and 2.2, respectively. The pK_a and n_H values from both two plots satisfactorily agree with those obtained from the pH/absorbance profile (Fig. 4b) and also with the previous data in ref [29]. Thus, these results indicate that the change of the hydration state of PA c551 (Fig. 6) takes place in a two-state transition alongside the acid unfolding of PA c551 which is also a two-state transition. Additionally, the pK_a and n_H values obtained from this analysis were little affected by the choice of the ϕ_A/c value in the range of 0.00217–0.00731 mL mg^{-1}.

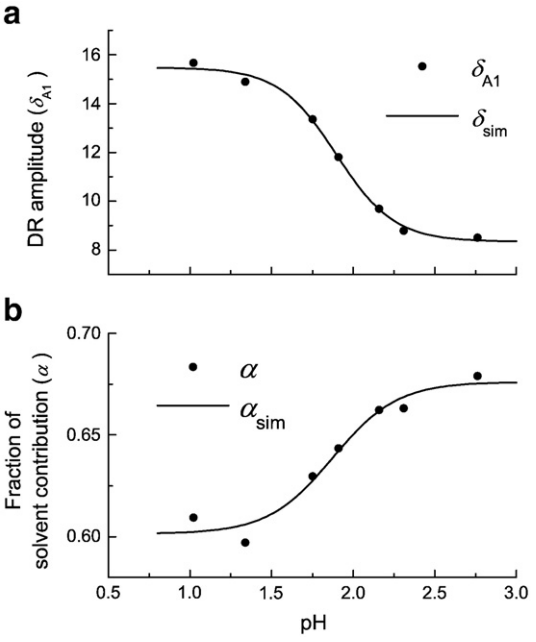

Fig. 6. Correlation between (a) the DR amplitude δ_{A1} and (b) the bulk solvent contribution α derived from the dielectric particle at a fixed volume per protein molecule and DR frequency. As a typical example, plots of the DR amplitude δ_{A1} and the bulk solvent contribution α were computed at ϕ_A /c = 0.0042 mL mg^{-1} and shown against pH. The δ_{sim} given by Eq. (9) was drawn as a function of pH using the pK_a and n_H values of 1.9 and 2.5, respectively, and α_{sim} given by Eq. (10), the pK_a and n_H values of 1.9 and 2.2, respectively.

3.5. Dependence of DR parameters on the model shape

Although the hydration analysis using the Wagner's dielectric mixture theory (Eq. (3)) allowed us to impartially analyze the DR property of the hydration water of PA c551 over the pH range of 1.0–6.2 (Figs. 5 and 6), the use of mixture theories for ellipsoidal dielectrics suspension may give a more precise description of the DR property of the hydration water in a particular conformational state than using the spherical shape as noted in Section 2.4. Thereby, the dielectric mixture theory for the suspension of randomly-oriented ellipsoids (Eq. (7)) [32,33], in place of Eq. (3), was also used to derive the DR spectrum $\varepsilon_q^*(f)$ of a particle containing a PA c551 molecule and its surrounding water, and the cross-recursive analysis was conducted to yield the DR parameters.

The shape of PA c551 in the native state seems nearly globular, according to X-ray crystallography study [24]. Thereby, the DR spectrum of aqueous PA c551 solution in the native state at pH 2.8 was examined with axial ratios ($q = R_z/R_x$, Section 2.4) around unity (Table 1). The result shows that the effect of the imposed shape of the solute particle on the DR parameters is so small that the variations of the DR parameters in the axial ratio range of 0.75–1.5 are almost within the experimental error at pH 2.8 (Fig. 5a,b,d).

In contrast, the conformation of the polypeptide chain in the acid unfolded state is thought to be randomly-coiled and extended to some degree. In the dielectric mixture theory given by Eq. (7), the dielectric particle containing an unfolded protein molecule and surrounding water was approximated with a dielectric ellipsoid of randomly-oriented as shown in Fig. 7. Thus, the hydration water/bulk water boundary of acid-unfolded PA c551 at pH 1.0 was determined, assuming that PA c551 is a prolate spheroid of axial ratio of 2–10 (Table 1). Even higher axial ratios (e.g., 100) were also examined, but

Table 1
DR parameterization of the DR spectra of PA c551 solutions determined by the procedures in Sections 2.3–2.4[a].

	c (mg mL^{-1})	s_v (g mL^{-1})	Axial ratio (R_z/R_x)	ϕ_{HB}/c (mg^{-1} mL)	$f_{c,HB}$ (GHz)	δ_{HB}	N_{hyd}	$f_{c,B}$ (GHz)	δ_B	σ (S m^{-1})[b]
pH 2.8	12.5	0.743	0.75	0.00103	4.63	21.9	147	0.23	4.0	0.52
(Native state)			1	0.00104	4.63	22.0	151	0.22	4.0	0.52
			1.5	0.00103	4.63	21.8	146	0.23	4.0	0.52
pH 1.0	12.2	0.711	2	0.00128	4.61	33.7	293	0.43	8.9	4.2
(Unfolded State)			4	0.00124	4.54	32.9	272	0.43	8.9	4.2
			10	0.00121	4.50	32.2	257	0.43	8.9	4.2
			100	0.00120	4.49	32.0	251	0.43	8.9	4.2

[a] The values were determined at $\phi_B/c = 0.00731$ mg^{-1} mL.
[b] The conductivity calculated by $\sigma = \sigma_0 + \Delta\sigma$ (see Eq. (2) and Supplementary material A2).

the DR parameters were changed very little with the increase of axial ratio q for $q \geq 10$. Thus, the differences between the DR parameters by the ellipsoid model and those by the spherical model are not significant. As shown in Table 1, the DR frequency $f_{c,HB}$ seems unchanged between the acid-unfolded and native conformations, but δ_{HB} and the number of hydration water molecules N_{hyd} increased by 1.7-fold upon acid unfolding. In addition, a 2.2-fold increase in the DR amplitude δ_B was detected as well.

4. Discussion

4.1. Identification of the dielectric dispersion around 5 GHz

By the least squares fitting analysis described in Section A3.2 of Supplementary material A3, the DR spectrum of an A-particle containing a PA c551 molecule and the surrounding water was able to be decomposed into a partial contribution of bulk solvent and one Debye relaxation function (Eq. (4)). The Debye-type relaxation component exhibited a DR frequency around 5 GHz in every condition examined in the present study. This DR component is thought to correspond to the δ_3 dispersion, according to ref [18], due to the reorientation of constrained water molecules, which constitute the largest part of the hydration shell of protein [12,13,18,37].

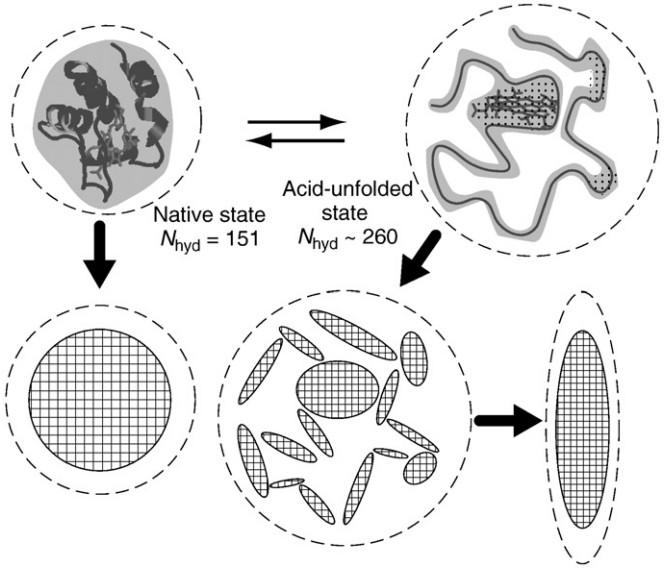

Fig. 7. Schematic diagram of hydrated PA c551 in the native and acid-unfolded states. In the native state a PA c551 molecule constrains 151 water molecules and ~260 in the acid-unfolded state. The illustration of the native state was generated using the structural data from the Protein Data Bank (451C). PA c551 in the acid-unfolded state is expected to have a 1.7-fold larger ASA than that in the native state, and is extended and flexible. Some amino acid residues in the acid-unfolded state would hydrophobically interact (depicted in dots), which likely contributes to its smaller ASA than that of the random-coil conformations. The peptide chain structure of the acid-unfolded state was drawn for schematic presentation purpose, and was modeled by n different ellipsoids. In the present analyses, one ellipsoid as having the total volume and the averaged dielectric property of n different ellipsoids was derived by the Eq. (7) instead of analyzing many different ellipsoids.

The DR analysis on a fixed volume containing a protein molecule (Section 3.4) must underpin the assignment of the dielectric dispersion around 5 GHz to the hydration water of PA c551. The analysis yielded the change of the DR amplitude δ_{A1} and the fraction of bulk solvent contribution α within the fixed-volume particle containing a PA c551 molecule as a function of pH in the range of pH 1–3 (Fig. 6). These two parameters were found to change oppositely with pH with each other: the low pH resulted in a high value of the DR amplitude δ_{A1} and a low value of the bulk solvent parameter α, and the high pH vice versa. This result indicates that some portion of the bulk water was transformed into the 5-GHz relaxation component, i.e., hydration water, upon acid unfolding of PA c551 within the particle of the fixed volume.

4.2. Accessible surface area and hydration number of PA c551

The DRS analysis of PA c551 hydration would also give an insight into the conformation of PA c551 in the acid-unfolded state. As shown in Table 1, the number of hydration water molecules N_{hyd} in the native state was derived to be 151 at $q = 1$, and that of acid-unfolded state 257 at $q = 10$. The increase of N_{hyd} upon acid unfolding must be due to an increase in the accessible surface area (ASA) of PA c551. The ASA of PA c551 in the native state was reported to be 4434 Å^2 according to ref [25]. As an approximation, if we assume that the ASA is proportional to the number of hydration water molecules and we can apply the ratio of ASA to the hydration number, 4434 (Å^2)/151 = 29.4 (Å^2/molecule), to the acid-unfolded state, the ASA of PA c551 in the unfolded state $ASA_{U,DRS}$ will be 7500 Å^2. In contrast, Oobatake and Ooi [38] derived a relationship between the ASA values of N and U states, which were deduced from, respectively, the Protein Data Bank and the ensemble averages of conformations covering possible dihedral angle for each residue:

$$ASA_{U,empirical} = ASA_N / (1.36 N_R^{-1/3}) = 14,200 \ \left(Å^2\right). \quad (11)$$

Interestingly, the $ASA_{U,DRS}$ of 7500 Å^2 derived from the DRS data is significantly smaller, suggesting that the acid-unfolded PA c551 must be of more compact conformation than fully extended polypeptide chain (Fig. 7), probably due to intramolecular hydrophobic interactions (dotted regions in Fig. 7).

4.3. On the dynamic processes for the dielectric dispersion around 0.2 GHz

A dielectric dispersion component around 0.2 GHz was also found in the DR spectra of PA c551 solutions (Fig. 5e,f). This dispersion exhibited an increase in the DR amplitude δ_B with decreasing pH for pH<3, and this change of δ_B was clearly accompanied by the increase of the DR amplitude of the hydration water δ_{HB} (Fig. 5b) upon acid unfolding of PA c551. Some DRS studies have reported a dielectric dispersion component at an order of 0.1 GHz for solutions of proteins such as ribonuclease A, myoglobin, and lysozyme [18,35], and suggested that this dielectric

dispersion may be attributed to the intramolecular fluctuation of the proteins. The change of the DR amplitude δ_B upon acid unfolding (Fig. 5f) seems consistent with the assignment of the dielectric dispersion component to the intramolecular fluctuation. It has been shown that the motion of ions surrounding a charged particle in an electrolyte solution can cause polarization when ac electric field is applied [33,39], and this is called the ion cloud relaxation. In the theory, its DR frequency was estimated by $f_c = D/2\pi R^2$, where D and R are, respectively, a mean diffusion coefficient of the ions (H^+, Na^+, HSO_4^- and SO_4^{2-} in this case) and a radius of the charged particle [34]. It will give a DR frequency of ~0.1 GHz for the PA c551 solutions with D and R taken from literatures [24,40]. Additionally, as stated in Section 4.2, the acid-unfolded PA c551 has a larger ASA than the native (Fig. 7), and this increased ASA may in turn cause an increase in the DR amplitude corresponding to the ion cloud relaxation, suggesting that the increase of δ_B upon acid unfolding (Fig. 5f) may be a manifestation of the change of ion cloud relaxation. The physical origin of the dielectric dispersion may not have been completely indentified, but the dielectric dispersion still likely reflects the conformational change of PA c551 and the resultant change in the motion and distribution of ions in the microenvironment of PA c551.

5. Conclusions

The analysis of the DR spectra between 3 and 26 GHz has revealed the hydration states of PA c551, whereas the analysis between 0.2 and 3 GHz has provided insights into the dynamic processes of PA c551 as well as its surrounding ions. The results from these analyses yielded information about the content of polarizable components in the PA c551 solution in relation to their dynamics, in particular, the mobility and the amount of the constrained water, i.e., the hydration water, of PA c551. Between pH 1 and 2.3, the hydration state of PA c551 changed in two-state transition alongside its acid unfolding, giving rise to the increase of the hydration water by 1.7-fold with the mobility of the hydration water almost unchanged. Between pH 2.3 and 6.2, PA c551 was still in the native state, but the mobility of the hydration water slightly increased with pH, which correlated with the ionization of the amino acid residues of the protein. Furthermore, the DR spectra in the low frequency region of <1 GHz are likely to be involved in the fluctuation dynamics and structural information of polypeptide chains of PA c551 and its microenvironment in aqueous solution. In the future, DRS study in combination with thermodynamics may resolve the enthalpic and entropic contributions of the hydration water and protein conformation to various processes in proteins. Thus, the analysis of aqueous protein solutions by DRS presented in this study is up for giving further insights into the protein-water interaction complementary to known methods such as CD, IR, Raman, and NMR spectroscopies.

Acknowledgment

We thank Prof. Satoshi Takahashi (Tohoku University) and Prof. Takao Kodama (Osaka University) for discussions and supports to the study, and Katsuhito Kambe (Tohoku University) for his assistance in the DRS study, Takafumi Sonoyama (Hiroshima University) for his assistance in the preparation of PA c551. This work was supported by grants from CREST/JST, and from the Ministry of Education, Culture, Sports, Science, and Technology of Japan (Grant-in-Aid for Scientific Research on Innovative Areas: 20118001, 20118005, 20118008, and GCOE Materials Integration Tohoku University).

Appendix A. Supplementary data

Supplementary data associated with this article can be found, in the online version, at doi:10.1016/j.bpc.2010.06.008.

References

[1] B. Halle, Protein hydration dynamics in solution: a critical survey, Phil. Trans. R. Soc. Lond. B. 359 (2004) 1207–1224.
[2] M. Nakasako, Water–protein interactions from high-resolution protein crystallography, Phil. Trans. R. Soc. Lond. B. 359 (2004) 1191–1206.
[3] N. Niimura, T. Chatake, K. Kurihara, M. Maeda, Hydrogen and hydration in proteins, Cell Biochem. Biophys. 40 (2004) 351–369.
[4] T.M. Raschke, Water structure and interactions with protein surfaces, Curr. Opinin. Sturct. Biol. 16 (2006) 152–159.
[5] T. Ooi, Thermodynamics of protein folding: effects of hydration and electrostatic interactions, Adv. Biophys. 30 (1994) 105–154.
[6] R. Buchner, G. Hefter, Interactions and dynamics in electrolyte solutions by dielectric spectroscopy, Phys. Chem. Chem. Phys. 11 (2009) 8984–8999.
[7] U. Kaatze, Y. Feldman, Broadband dielectric spectroscopy of liquids and biosystems, Meas. Sci. Technol. 17 (2006) R17–R35.
[8] T. Miyazaki, G. Mogami, T. Wazawa, T. Kodama, M. Suzuki, Measurement of the dielectric relaxation property of water-ion loose complex in aqueous solutions of salt at low concentrations, J. Phys. Chem. A. 112 (2008) 10801–10806.
[9] S. Takashima, Electrical Properties of Biopolymers and Membranes, Adam Hilger, Bristol, 1989.
[10] A. Bonincontro, G. Risuleo, Dielectric spectroscopy as a probe for the investigation of conformational properties of proteins, Spectrochim. Acta Part A. 59 (2003) 2677–2684.
[11] U. Kaatze, Complex permittivity of water as a function of frequency and temperature, J. Chem. Eng. Data. 34 (1989) 371–374.
[12] R. Pethig, Protein-water interactions determined by dielectric methods, Annu. Rev. Phys. Chem. 43 (1992) 177–205.
[13] M. Suzuki, J. Shigematsu, T. Kodama, Hydration study of proteins in solution by microwave dielectric analysis, J. Phys. Chem. 100 (1996) 7279–7282.
[14] E.H. Grant, B.G.R. Mitton, G.P. South, R.J. Sheppard, An investigation by dielectric methods of hydration in myoglobin solutions, Biochem. J. 139 (1974) 375–380.
[15] H.-J. Steinhoff, B. Kramm, G. Hess, C. Owerdieck, A. Redhardt, Rotational and translational water diffusion in the hemoglobin hydration shell: dielectric and proton nuclear relaxation measurements, Biophys. J. 65 (1993) 1486–1495.
[16] Y.-Z. Wei, A.C. Kumbharkhane, M. Sadeghi, J.T. Sage, W.D. Tian, P.M. Champion, S. Sridhar, Protein hydration investigations with high-frequency dielectric spectroscopy, J. Phys. Chem. 98 (1994) 6644–6651.
[17] K. Yokoyama, T. Kamei, H. Minami, M. Suzuki, Hydration study of globular proteins by microwave dielectric spectroscopy, J. Phys. Chem. B. 105 (2001) 12622–12627.
[18] A. Oleinikova, P. Sasisanker, H. Weingärtner, What can really be learned from dielectric spectroscopy of protein solutions? A case study of ribonuclease A, J. Phys. Chem. B. 108 (2004) 8467–8474.
[19] A. Knocks, H. Weingärtner, The dielectric spectrum of ubiquitin in aqueous solution, J. Phys. Chem. B. 105 (2001) 3635–3638.
[20] S.R. Kabir, K. Yokoyama, K. Mihashi, T. Kodama, M. Suzuki, Hyper-mobile water is induced around actin filaments, Biophys. J. 85 (2003) 3154–3161.
[21] M. Suzuki, S.R. Kabir, M.S.P. Siddique, U.S. Nazia, T. Miyazaki, T. Kodama, Myosin-induced volume increase of the hyper-mobile water surrounding actin filaments, Biochem. Biophys. Res. Comm. 322 (2004) 340–346.
[22] T. Kamei, M. Oobatake, M. Suzuki, Hydration of apomyoglobin in native, molten globule, and unfolded states by using microwave dielectric spectroscopy, Biophys. J. 82 (2002) 418–425.
[23] Y. Sambongi, S. Uchiyama, Y. Kobayashi, Y. Igarashi, J. Hasegawa, Cytochrome *c* from a thermophilic bacterium has provided insights into the mechanisms of protein maturation, folding, and stability, Eur. J. Biochem. 269 (2002) 3355–3361.
[24] Y. Matsuura, T. Takano, R.E. Dickerson, Structure of cytochrome *c*551 from *Pseudomonas aeruginosa* refined at 1.6 Å resolution and comparison of the two redox forms, J. Mol. Biol. 156 (1982) 389–409.
[25] J. Hasegawa, H. Shimahara, M. Mizutani, S. Uchiyama, H. Arai, M. Ishii, Y. Kobayashi, S.J. Ferguson, Y. Sambongi, Y. Igarashi, Stabilization of *Pseudomonas aeruginosa* cytochrome *c*(551) by systematic amino acid substitutions based on the structure of thermophilic *Hydrogenobacter thermophilus* cytochrome *c*(552), J. Biol. Chem. 274 (1999) 37533–37537.
[26] J. Hasegawa, S. Uchiyama, Y. Tanimoto, M. Mizutani, Y. Kobayashi, Y. Sambongi, Y. Igarashi, Selected mutations in a mesophilic cytochrome *c* confer the stability of a thermophilic counterpart, J. Biol. Chem. 275 (2000) 37824–37828.
[27] T. Sonoyama, J. Hasegawa, S. Uchiyama, S. Nakamura, Y. Kobayashi, Y. Sambongi, Stability enhancement of cytochrome c through heme deprotonation and mutations, Biophys. Chem. 139 (2009) 37–41.
[28] S. Gianni, C. Travaglini-Allocatelli, F. Cutruzzola, M.G. Bigotti, M. Brunori, Snapshots of protein folding. A study on the multiple transition state pathway of cytochrome *c*551 from *Pseudomonas aeruginosa*, J. Mol. Biol. 309 (2001) 1177–1187.
[29] M.G. Bigotti, C.T. Allocatelli, R.A. Staniforth, M. Arese, F. Cutruzzolà, M. Brunori, Equilibrium unfolding of a small bacterial cytochrome, cytochrome *c*551 from *Pseudomonas aeruginosa*, FEBS Lett. 425 (1998) 385–390.
[30] U. Kaatze, R. Pottel, On a hydration model utilized in the discussion of dielectric spectra of aqueous solutions, J. Mol. Liq. 30 (1985) 115–131.
[31] K.W. Wagner, Erklärung der dielektrischen Nachwirkungsvorgänge auf Grund Maxwellscher Vorstellungen, Arch. Electrotech. 2 (1914) 371–387.
[32] K. Asami, T. Hanai, N. Koizumi, Dielectric approach to suspensions of ellipsoidal particles covered with a shell in particular reference to biological cells, Jpn. J. Appl. Phys. 19 (1980) 359–365.

[33] K. Asami, Characterization of heterogeneous systems by dielectric spectroscopy, Prog. Polym. Sci. 27 (2002) 1617–1659.
[34] C. Grosse, K.R. Foster, Permittivity of a suspension of charged spherical particles in electrolyte solution, J. Phys. Chem. 91 (1987) 3073–3076.
[35] I.V. Ermolina, V.D. Fedotov, Y.D. Feldman, Structure and dynamic behavior of protein molecules in solution, Physica A. 249 (1998) 347–352.
[36] P.A. Adams, D.A. Baldwin, H.M. Marques, Cytochrome *c*: A multidisciplinary approach, in: R.A. Schott, A.G. Mauk (Eds.), The hemepeptides from cytochrome c: preparation, physical and chemical properties, and their use as model compounds for the hemoproteins, University Science Books, Sausalito, CA, 1996, p. 635.
[37] U. Kaatze, On the existence of bound water in biological systems as probed by dielectric spectroscopy, Phys. Med. Biol. 35 (1990) 1663–1681.
[38] M. Oobatake, T. Ooi, Hydration and heat stability effects on protein unfolding, Prog. Biophys. Molec. Biol. 59 (1993) 237–284.
[39] C. Grosse, A.V. Delgado, Dielectric dispersion in aqueous colloidal systems, Curr. Opinin. Colloid Interface Sci. 15 (2009) 145–159.
[40] D.R. Lide, CRC Hamdbook of Chemistry and Physics, 79th Ed.CRC Press, Boca Raton, FL, 1998.